Magnetization reversal in permalloy ferromagnetic nanowires investigated with magnetoresistance measurements

A. B. Oliveira,* S. M. Rezende, and A. Azevedo
Departamento de Física, Universidade Federal de Pernambuco, 50670-901, Recife, Pernambuco, Brazil
(Received 20 March 2008; published 21 July 2008)

The magnetization reversal process in single Permalloy ($Ni_{81}Fe_{19}$) nanowires has been investigated by magnetoresistance measurements as a function of the angle between the applied field and the wire direction. The Permalloy nanostructures fabricated on an ultrathin film by atomic force microscopy consist of two large rectangular pads connected by a nanowire with the shape of a long thin narrow tape. For each field direction in the plane of the film the dependence of the magnetoresistance on the field value exhibits two main contributions: one from the pads and one from the nanowire. The contribution from the pads is due to a usual anisotropic magnetoresistance characteristic of coherent magnetization rotation, whereas the contribution from the nanowire is an abrupt transition at the switching field. The dependence of the switching field on the in-plane field angle is quantitatively described by a model of nucleation field with the buckling magnetization rotation mode.

DOI: 10.1103/PhysRevB.78.024423 PACS number(s): 75.75.+a, 75.47.−m

I. INTRODUCTION

The understanding and control of the magnetization reversal processes in patterned nanoscale magnetic structures has been the subject of considerable interest in recent years due to the emergence of novel size-dependent magnetic effects and their potential application in magnetoelectronic devices.[1,2] Among these structures the magnetic nanowires have attracted particular attention because of the possibility of their fabrication with a very large areal density. From the experimental point of view, anisotropic magnetoresistance (AMR) (Ref. 3) measurements have been shown to be a very sensitive technique to investigate magnetization reversal processes as well as the domain-wall structure in magnetic nanoscale systems.[4] In such experiments the ferromagnetic sample is saturated by a strong magnetic field applied along a certain direction. As the magnetic-field value is scanned and eventually reversed, an instability of the magnetization usually occurs at a critical-field value, leading to a magnetization reversal. The angular dependence of the switching field is compared to the predictions of theoretical models in order to draw conclusions about the micromagnetic origin of the magnetization reversal process. Although theoretical efforts have elucidated most of the features that go along with the magnetization reversal in nanoscale elements, important questions remain open regarding the micromagnetic origin of the reversal process in constrained structures with nonellipsoidal shape.

In this paper we report the results of experimental and theoretical investigations of the magnetization reversal process in magnetic nanowires with the shape of a long thin narrow tape. We use magnetoresistance measurements to characterize the magnetization reversal process and show that the angular dependence of the switching field is quantitatively explained by a model of nucleation dominated by an oscillatory buckling mode for the magnetization. Previously published papers support that the switching of the magnetization in nanowires is dominated by a curling reversal mode,[5] which is probably valid for cylindrical geometries[6,7] but not for tapes[8] as shown in the current investigation. The paper is organized as follows: Section II presents details of the fabrication and characterization of the nanowires used in this investigation and the data of the angular dependence of the switching fields in two samples. Section III presents the theory for the oscillatory buckling mode of the magnetization in a nanowire with the shape of a long thin narrow tape. Section IV is devoted to the comparison between theory and experimental data and Sec. V summarizes the investigation.

II. EXPERIMENTAL DETAILS AND MEASUREMENTS

We have investigated magnetization reversal processes in several structures consisting of two rectangular pads measuring 70×80 μm^2, which are connected by a 5–10-μm-long nanowire having widths in the range of 300–400 nm and fabricated on Permalloy (Py) films with thickness in the range of 3–10 nm. Atomic force microscopy (AFM) has been used to fabricate the nanostructures. A 30-nm-thick film of Polymethylmethacrylate (PMMA) of high molecular weight (996 000 g/mol) is spin coated at 5000 rpm on top of oxidized Si substrate from a 1.0 wt % solution in anisole. The nanostructure pattern is mechanically transferred to the resist film of PMMA by scratching the AFM tip on the resist film surface.[9] A Py ($Ni_{81}Fe_{19}$) film is then deposited by sputtering on the patterned sample. To prevent oxidation a SiO_2 layer of 1 nm thickness is deposited on top of the Py structure. In order to remove the PMMA left over, the sample is finally soaked in an ultrasonic acetone bath for a few minutes and then dried under nitrogen flow. In order to make the macroscopic contact with silver painting, palladium pads measuring 3×3 mm^2 are sputtered before the spin-coating step. An illustration of the final structure is shown in Fig. 1(a) and a scanning electron microscopy (SEM) image of the magnetic part of one of the samples is presented in Fig. 1(b).

Magnetoresistance (MR) measurements were carried out at room temperature using a direct current (dc) of 200 μA passing through the Pd pads and the Py nanowire and sweeping the external magnetic field applied in the plane of the

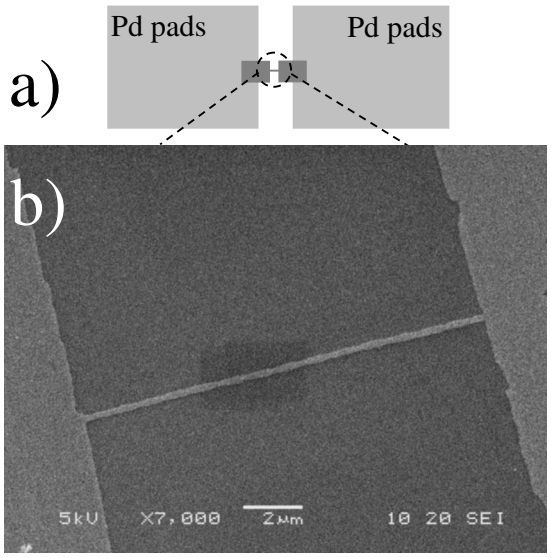

FIG. 1. (a) Schematic of the nanostructures used in this investigation. The two Pd pads (light gray) measuring 3×3 mm^2 were used as the electrodes to apply the current for the MR measurements. The ferromagnetic structure is illustrated in dark gray. (b) SEM image of a ferromagnetic nanostructure of Py consisting of two rectangular pads measuring 70×80 mm^2 connected by a Py nanowire having length of 12 μm, width of 290 nm, and thickness of 12 nm.

sample. Figure 2 shows a typical MR data obtained with the external magnetic field applied parallel to the wire axis. The magnetic-field dependence of the measured resistance is clearly a superposition of a continuous variation corresponding to a reversible rotation of the magnetization and discontinuous jumps attributed to irreversible magnetization switching. The magnetic-field up-sweep MR data shown by the solid line in Fig. 2 exhibits three magnetization regimes as described in the next paragraph: (a) A coherent rotation of the magnetization in the macroscopic pads (region 2); (b) pinning and depinning of the domain walls that separate the nanowire magnetization region from the pads magnetization regions (see the downward steps shown in region 3 of Fig. 2); and (c) switching process of the nanowire magnetization that occurs within a very narrow range of magnetic field where the magnetization of the nanowire reverses completely (between regions 3 and 4).

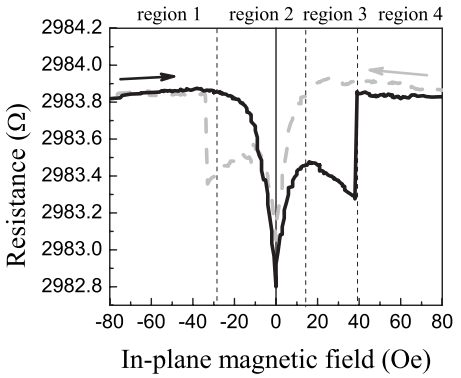

FIG. 2. Longitudinal MR for the structure described in Fig. 1(b) as a function of the applied magnetic field. The up-field sweep (solid line) exhibits four different regimes of magnetization states. The switching field is characterized by the abrupt change occurring at 40 Oe.

We will concentrate our analysis on the MR variation obtained with the up sweep of the magnetic field applied along the wire axis shown by the solid line in Fig. 2 and characterized by the four regions: (i) In region 1 ($-80<H<-30$ Oe), the magnetizations of both Py pads and Py nanowire are saturated resulting in an essentially constant MR signal; (ii) in the middle of region 2 ($-30<H<13$ Oe), the MR variation shows a continuous negative reversible peak near zero field attributed to the magnetization reversal of the pads. This behavior is typical of the AMR when the current is parallel to the magnetic field applied in the film plane, in which the magnetization reverses by coherent rotation as described by the Stoner-Wohlfarth model.[10] In this case AMR$\propto\cos^2(\phi_M-\phi_I)$, where ϕ_M and $\phi_I(=0°)$ are, respectively, the angles that the pads magnetizations and current direction make with the wire axis. The minimum (corresponding to $\phi_M=90°$) occurs at a field value near zero as expected for the low coercivity Py macroscopic pads; (iii) in region 3 ($13<H<38$ Oe), the MR data show a series of down steps, which we attribute to domain-wall movements at the interface between the nanowire and the pads where the magnetization has to overcome local pinning barriers; and (iv) finally, in region 4, ($H>40$ Oe), there is an abrupt transition to a plateau where the constant MR indicates that saturation has been achieved and the magnetization of the whole structure has been reversed. The abrupt transition characterizes the switching of the magnetization in the long nanowire. As it will be shown in the remainder of this paper, the switching of the magnetization in the nanowire has a nucleation with the buckling instability mode.

In order to compare theory with experiments, we measured the MR varying the direction of the applied field in the film plane. Typical magnetoresistive hysteresis loops obtained in the same sample of Fig. 2 are shown in Fig. 3 for three different in-plane angles. As the pads hystereses are negligible, the hysteresis behavior observed in all of MR curves is due to the irreversible rotation of the nanowire magnetization. As observed by other authors,[6–8,11] the switching field (H_{sw}) values, indicated by the arrows, exhibit a significant dependence with the angle ϕ_H between the field and the direction of the nanowire. Figures 4(a) and 4(b) show detailed measurements (data are shown by the empty circles) of H_{sw} versus ϕ_H for two different samples with dimensions described in the captions. Although the data can be well fitted by the equations derived for the curling nucleation mode, we noticed that in this case the extracted physical parameters are completely unrealistic. For instance, if we fit Eq. (12) of Ref. 5 for the curling mode to the data of Fig. 4(a) with demagnetizing factors as adjustable parameters, we obtain $D_x=D_y=0.341$ and $D_z=0.318$. These values correspond approximately to a spherical sample, which does not make sense in comparison with our rectangular nanowires. Actually the appropriate test of how good is our interpretation is given by the extracted physical parameters. The U-shape curves symmetric around $H=0$ shown by the solid lines in Figs. 4 are obtained with a calculation for the buckling mode described in Sec. III.

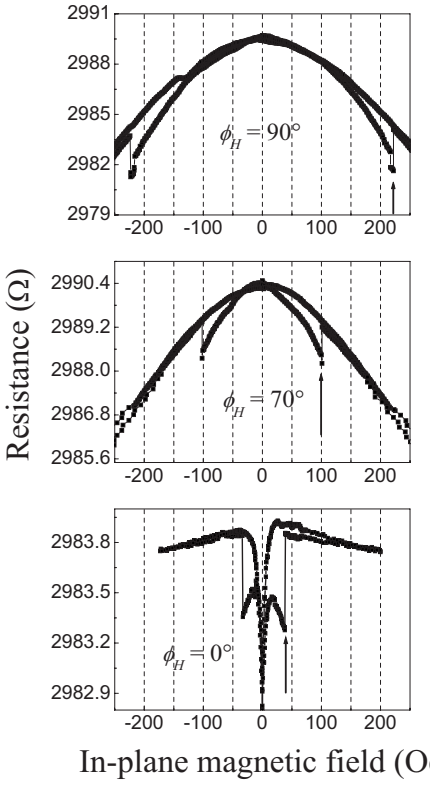

FIG. 3. Magnetoresistance hysteresis obtained at three different in-plane field angles for the same sample of Fig. 2. Arrows indicate the switching field values.

III. THEORETICAL MODEL

The problem of magnetization reversal in confined geometries that reappeared in the last decade is mainly due to the feasibility of fabrication and characterization of single nanostructures.[6–8,11] Some of the investigated nanostructures are patterned nanowires with the shape of long narrow thin tapes, but the theoretical models used to interpret the measurements are based on the nucleation theory developed for ellipsoidal geometries.[5,12,13] This approach led to unexpected physical results, and the parameters obtained by the numerical fittings to the experimental data are nonrealistic. Nucleation theory proposes that the magnetization reversal occurs by three different modes: coherent rotation, curling, and buckling. Coherent rotation and curling modes can be analytically solved for some special nanostructure shapes such as ellipsoids of revolution. On the other hand, magnetization reversal by buckling mode has only been considered in theoretical numerical analysis.[14]

Due to the rectangular geometry, magnetic nanowires of rectangular cross section should be expected to exhibit a magnetization reversal mode different from curling or coherent rotation. This is so because both these modes create uncompensated magnetic poles along the nanowire edges, which increase the magnetostatic energy. Here we propose that the nucleation mode for the instability in rectangular cross-section nanowires is the oscillatory magnetization buckling mode that has been theoretically investigated recently.[14,15]

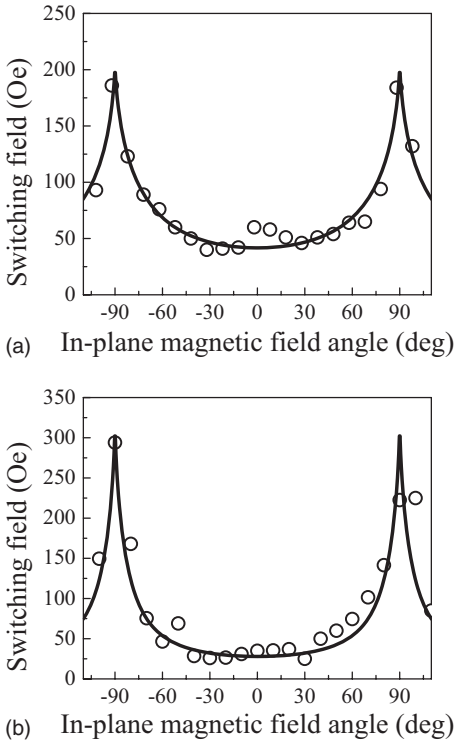

FIG. 4. Switching field of Py nanowires as a function of the in-plane angle. The open circles represent the experimental data measured by MR and the solid lines are the fits with the theoretical model for the nucleation field using the magnetization buckling mode. The calculations for the two samples were done with the following parameters: (a) Geometrical parameters: length=10 μm, width=460 nm and thickness=3.5 nm. Fitting parameters: $N_{x'}=4\pi\times0.023$ and $N_{z'}=0$; and (b) geometrical parameters: length=6 μm, width=290 nm and thickness=12 nm. Fitting parameters: $N_{x'}=4\pi\times0.036$ and $N_{z'}=0$. As discussed in the text $n=27$ and $n=13$ for Figs. 4(a) and 4(b), respectively.

Before nucleation, the magnetization vector $\vec{M}$ is assumed to undergo a coherent rotation to stay in equilibrium at an angle $\phi_{M,0}$ with the nanowire direction. Taking into account only the Zeeman and shape contributions to the magnetic energy and considering the geometry and coordinate system shown in Fig. 5(a), the minimization of the total energy results in

$$H_a \sin(\phi_H - \phi_{M,0}) = \frac{1}{2} M_S (N_{x'} - N_{z'}) \sin(2\phi_{M,0}), \qquad (1)$$

where ϕ_H is the in-plane angle of the applied magnetic field (H_a) with respect to the wire axis, M_S is the saturation magnetization, and $N_{x'}$ and $N_{z'}$ are the normalized demagnetizing factor for x' and z' directions, respectively. As shown in Fig. 5(a), two coordinate systems are used: the $x'y'z'$ system is fixed with respect to the nanowire axis and the x, y, and z coordinates rotate with the magnetization with the z axis pointing along $\vec{M}$.

In order to calculate the nucleation field, one has to solve the linearized Brown's equations.[5,12,13] Just before nucleation, the magnetization is aligned along the equilibrium di-

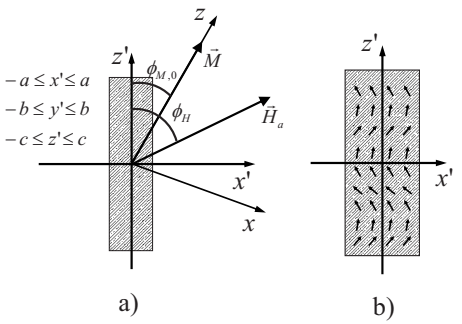

FIG. 5. (a) Coordinates systems used in the nucleation field theory calculation. (b) Illustration of the buckling rotation mode used to describe the magnetization state at the beginning of the nucleation.

rection so that $\vec{M}=M_S\hat{z}$. At nucleation the magnetization deviates from equilibrium and is described by small components perpendicular to the z direction; m_x and m_y. The free-energy variational problem is solved such that, at a minimum configuration, the variation of the total energy should vanish. The small magnetization components are described by the following differential equations:[5,12,13]

$$C\nabla^2 m_x + M_S(H_x - m_x H_z) = 0, \tag{2a}$$

and

$$C\nabla^2 m_y + M_S(H_y - m_y H_z) = 0. \tag{2b}$$

Neglecting surface anisotropy contribution, the boundary conditions on the surface of the nanowire is

$$\frac{\partial \vec{M}}{\partial n} = 0, \tag{3}$$

where $\hat{n}$ is a unit vector normal to the structure surface, C is the exchange constant, $\vec{m}=\vec{M}/M_S$ is the normalized magnetization of the system, and (H_x,H_y,H_z) are components of the total internal magnetic field that includes applied and magnetostatic fields. It is important to notice that Eqs. (2) were derived for the xyz-coordinate system, which has its z direction parallel to $\vec{M}$ before nucleation. For the sake of simplicity we took into account only the demagnetizing and Zeeman energies in order to find the nucleation field condition. Then the components of the total magnetic field can be written as

$$\begin{aligned} H_x &= H_x^a + H_x^{\text{demag}} \\ &= H_a \sin(\phi_H - \phi_{M,0}) \\ &\quad + (H_{x'}^{\text{demag}} \cos\phi_{M,0} - H_{z'}^{\text{demag}} \sin\phi_{M,0}), \end{aligned} \tag{4a}$$

$$\begin{aligned} H_z &= H_z^a + H_z^{\text{demag}} \\ &= H_a \cos(\phi_H - \phi_{M,0}) \\ &\quad + (H_{x'}^{\text{demag}} \sin\phi_{M,0} + H_{z'}^{\text{demag}} \cos\phi_{M,0}), \end{aligned} \tag{4b}$$

$$H_y = H_y^a + H_y^{\text{demag}} = H_{y'}^{\text{demag}}. \tag{4c}$$

Here we assume that the demagnetizing field inside the nanowire is uniform and has the components $H_{x'}^{\text{demag}} = -N_{x'}M_S \sin\phi_{M,0}$, $H_{z'}^{\text{demag}} = -N_{z'}M_S \cos\phi_{M,0}$, and $H_{y'}^{\text{demag}} = 0$. This last term is zero, because we consider that the out-of-plane magnetization component is negligible. So Eqs. (4) can be rewritten as

$$H_x = H_a \sin(\phi_H - \phi_{M,0}) + M_S(N_{z'} - N_{x'})\sin(\phi_{M,0})\cos(\phi_{M,0}), \tag{5a}$$

$$\begin{aligned} H_z &= H_a \cos(\phi_H - \phi_{M,0}) \\ &\quad - M_S[N_{x'} \sin^2(\phi_{M,0}) + N_{z'} \cos^2(\phi_{M,0})], \end{aligned} \tag{5b}$$

$$H_y = 0. \tag{5c}$$

It is more convenient to solve Eqs. (2) and interpret the magnetization rotation in the $x'y'z'$ coordinate system. So we perform the following coordinate system transformation:

$$m_x = m_{x'} \cos\phi_{M,0} - m_{z'} \sin\phi_{M,0}, \tag{6a}$$

$$m_z = m_{x'} \sin\phi_{M,0} + m_{z'} \cos\phi_{M,0}, \tag{6b}$$

$$m_y = m_{y'}. \tag{6c}$$

As mentioned earlier, our model is based on the assumption that the magnetization of the nanowire is in the x-z plane, so we only need to solve Eq. (2a) to calculate the nucleation field. Inserting Eqs. (5a), (5b), (6a), and (6b) into Eq. (2a) and neglecting second-order terms in m_x we obtain,

$$\begin{aligned} &C\cos\phi_{M,0}\left[\cos^2(\phi_{M,0})\frac{\partial^2}{\partial x'^2} + \frac{\partial^2}{\partial y'^2} + \cos^2(\phi_{M,0})\frac{\partial^2}{\partial z'^2}\right] m_{x'} \\ &\quad + M_S\{H_a \sin(\phi_H - \phi_{M,0}) + M_S(N_{z'} \\ &\quad - N_{x'})\sin(\phi_{M,0})\cos(\phi_{M,0}) - [m_{x'} \cos(\phi_{M,0}) - \sin(\phi_{M,0})] \\ &\quad \times [H_a \cos(\phi_H - \phi_{M,0}) - M_S(N_{x'} \sin^2\phi_{M,0} \\ &\quad + N_{z'} \cos^2\phi_{M,0})]\} = 0. \end{aligned} \tag{7a}$$

The above equation can be simplified by making a linear transformation given by $m_{x'} \to m_{x'} + \lambda$, which for an appropriate choice of λ, leaves the eigenvalues unaffected. After the transformation Eq. (7a) can be written as

$$\begin{aligned} &C\cos(\phi_{M,0})\left[\cos^2(\phi_{M,0})\frac{\partial^2}{\partial x'^2} + \frac{\partial^2}{\partial y'^2} + \cos^2(\phi_{M,0})\frac{\partial^2}{\partial z'^2}\right] m_{x'} \\ &\quad - M_S \cos(\phi_{M,0})[H_a \cos(\phi_H - \phi_{M,0}) + M_S(N_{x'} \sin^2\phi_{M,0} \\ &\quad + N_{z'} \cos^2\phi_{M,0})]m_{x'} - M_S \cos(\phi_{M,0})[H_a \cos(\phi_H \\ &\quad - \phi_{M,0}) + M_S(N_{x'} \sin^2\phi_{M,0} + N_{z'} \cos^2\phi_{M,0})]\lambda \\ &\quad + M_S[H_a \sin(\phi_H - \phi_{M,0}) + M_S(N_{z'} \\ &\quad - N_{x'})\sin(\phi_{M,0})\cos(\phi_{M,0})] + M_S \sin(\phi_{M,0})[H_a \cos(\phi_H \\ &\quad - \phi_{M,0}) + M_S(N_{x'} \sin^2\phi_{M,0} + N_{z'} \cos^2\phi_{M,0})] = 0. \end{aligned} \tag{7b}$$

By appropriate choice of λ, the sum of last three terms can be made null, so that Eq. (7b) becomes

$$C\left[\cos^2(\phi_{M,0})\frac{\partial^2}{\partial x'^2}+\frac{\partial^2}{\partial y'^2}+\cos^2(\phi_{M,0})\frac{\partial^2}{\partial z'^2}\right]m_{x'} - M_S m_{x'}[H_a\cos(\phi_H-\phi_{M,0})- M_S(N_{x'}\sin^2\phi_{M,0} + N_{z'}\cos^2\phi_{M,0})]=0\ . \quad (8)$$

Finally, it is necessary to choose the type of magnetization rotation mode among the possible solutions $m_{x'}(x',y',z')$ of Eq. (8). Due to the confined lateral nanowire dimension we do not expect the mode to be either the coherent rotation or the curling, because both types create large demagnetizing fields. The rotation mode we consider here is the oscillatory buckling one, which is illustrated in Fig. 5(b). This mode is characterized by a x' component of the magnetization given by

$$m_{x'}=A\sin(kz'), \quad (9)$$

where A is a constant amplitude and k is the wave number associated with the buckling. Due to the boundary condition of Eq. (3) the wave number k assumes discreet values given by

$$k=(2n+1)\frac{\pi}{2c}, \quad (10)$$

where $n=0,1,2,\ldots$ and c is half of the nanowire's length. Considering that just before switching the magnetization instability is given by Eq. (9), the equation that describes the nucleation field for a rectangular nanowire can be obtained by using Eq. (9) in Eq. (8). This leads to

$$-k^2C\cos^2\phi_{M,0}-M_S H_{nuc}\cos(\phi_H-\phi_{M,0}) + M_S^2(N_{x'}\sin^2\phi_{M,0}+N_{z'}\cos^2\phi_{M,0})=0, \quad (11)$$

where H_{nuc} denotes the nucleation field as the value of the applied field H_a that is a solution of Eq. (11). This is the main result of the theory for the nucleation with the buckling mode. Note that k given by Eq. (10) may have an infinite number of values, so it should be given appropriate consideration. If we follow the arguments presented by Aharoni[5] and choose the value of k that results in a less negative nucleation field, this should be $k=\pi/2c$. However, if we calculate the nucleation field using Eq. (11) for the field applied along the nanowire axis, i.e., $\phi_H=0\Rightarrow\phi_{M,0}=0$ and assuming that demagnetizing field is negligible along the z' direction, (according to the coordinate system shown in Fig. 5, $N_{z'}=0$) we obtain

$$H_{\mathrm{nuc}}(\phi_H=0)=-\frac{k^2C}{M_S}. \quad (12)$$

Therefore, instead of using $k=\pi/2c$, we use for the wave number k a value determined from Eq. (12) with the experimental value of $H_{\mathrm{nuc}}(\phi_H=0)$, using the known values for the exchange constant C and saturation magnetization M_S for the material. In order to calculate the value of n from Eq. (10) we first use Eq. (12) to obtain k and substitute it in Eq. (10) and then we choose the nearest integer that provides the best fit to the experimental data.

IV. COMPARISON WITH EXPERIMENTAL MEASUREMENTS

In order to test the theory for nucleation with the buckling mode, we compare the results of the calculation presented in Sec. III with the measured angular dependence of the switching fields in two different nanowires of Py as shown in Fig. 4. Figure 4(a) shows the measured switching field values (open circles) as a function of the in-plane field angle for a nanowire that is 6.0 μm long, 290 nm wide, and 12 nm thick. Figure 4(b) shows the data for another nanowire that is 10 μm long, 460 nm wide, and 3.5 nm thick. Since the physical parameters are extracted from the numerical fitting, the investigation of samples with quite different dimensions is relevant to provide support to our theoretical model proposition as discussed below.

In order to calculate the nucleation field H_{nuc} for an arbitrary angle of the applied field, one has to obtain the equilibrium angle $\phi_{M,0}$ from Eq. (1) and use it in Eq. (11). Of course, since the solution of Eq. (1) depends on the applied field, Eqs. (1) and (11) have to be solved simultaneously. The solid lines in Figs. 4(a) and 4(b) were obtained by numerical solution of Eqs. (1) and (11) considering $4\pi M_S=9000$ G and $C=10^{-6}$ erg/cm. The other parameters used in the calculation are given in the caption of Fig. 4. As expected the demagnetizing factor for the y' direction ($N_{y'}=4\pi-N_{x'}$) is very close to 4π in both cases, because the thickness of the nanowire tape is smaller than its width by more than one order of magnitude. In addition note that as the width of nanowire increases, the demagnetizing factor $N_{x'}$ decreases as expected from the behavior of the demagnetizing field. Another important result to note is that as the length of nanowire decreases by half, the wave number also decreases approximately by half. This is a strong indication of the relation between the length of nanowire and the wave number of the buckling rotation mode.

V. SUMMARY

We have presented the results of an investigation of magnetization reversal in ferromagnetic nanowires fabricated by means of mechanical lithography using atomic force microscopy. The samples have structures consisting of two rectangular pads measuring 70×80 μm^2 connected by a 5–10-μm-long nanowire having widths in the range 300–400 nm and fabricated on Py films with thickness in the range 3–10 nm. The magnetization reversal in the nanowires is identified by a switching field characterized by an abrupt

change in the magnetoresistance measured with field sweeping. The angular dependencies of the switching fields in two samples are quantitatively explained by a model of nucleation dominated by an oscillatory buckling mode for the magnetization.

ACKNOWLEDGMENTS

The authors acknowledge the financial support by the Brazilian federal agencies; CNPq, FINEP, and CAPES; and the Pernambuco state agency FACEPE.

*Corresponding author. abo@df.ufpe.br

[1] D. A. Allwood, G. Xiong, C. C. Faulkner, D. Atkinson, D. Petit, and R. P. Cowburn, Science **309**, 1688 (2005).
[2] M. Hayashi, L. Thomas, C. Rettner, R. Moriya, and S. S. P. Parkin, Nat. Phys. **3**, 21 (2007).
[3] T. R. McGuire and R. I. Potter, IEEE Trans. Magn. **11**, 1018 (1975).
[4] K. Hong and N. Giordano, J. Magn. Magn. Mater. **151**, 396 (1995).
[5] A. Aharoni, J. Appl. Phys. **82**, 1281 (1997).
[6] J.-E. Wegrowe, D. Kelly, A. Franck, S. E. Gilbert, and J.-Ph. Ansermet, Phys. Rev. Lett. **82**, 3681 (1999).
[7] S. Pignard, G. Goglio, A. Radulescu, L. Piraux, S. Dubois, A. Declemy, and J. L. Duvail, J. Appl. Phys. **87**, 824 (2000).
[8] A. O. Adeyeye, R. P. Cowburn, and M. E. Welland, J. Appl. Phys. **87**, 299 (2000).
[9] Yu-Ju Chen, Ju-Hung Hsu, and Heh-Nan Lin, Nanotechnology **16**, 1112 (2005).
[10] E. C. Stoner and E. P. Wohlfart, Philos. Trans. R. Soc. London, Ser. A **240**, 599 (1948).
[11] Y. Rheem, B.-Y. Yoo, W. P. Beyermann, and N. V. Myung, Nanotechnology **18**, 125204 (2007).
[12] W. F. Brown, Jr., Phys. Rev. **105**, 1479 (1957).
[13] A. Aharoni, *Introduction to the Theory of Ferromagnetism*, 2nd ed. (Oxford Science/Oxford University Press, New York, 2000).
[14] N. A. Usov, Ching-Ray Chang, and Zung-Hang Wei, Phys. Rev. B **66**, 184431 (2002).
[15] R. Cantero-Alvarez and F. Otto, J. Nonlinear Sci. **16**, 351 (2006).